ANL/ET/CP--89773

CONF-9605167--2

EFFECTS OF FLAWS ON FRACTURE BEHAVIOR OF STRUCTURAL CERAMICS*

J. P. Singh, D. Singh, and M. Sutaria
Energy Technology Division
Argonne National Laboratory
Argonne, IL 60439

May 1996

DISCLAIMER

To be published in Proceedings of 10th Annual Conference on Fossil Energy Materials, Knoxville, TN, May 14-16, 1996.

*Research sponsored by the Office of Fossil Energy, Advanced Research and Technology Development Materials Program [DOE/FE AA 15 10 10 0, Work Breakdown Structure Element ANL-1], U.S. Department of Energy, under Contract W-31-109-Eng-38.

EFFECTS OF FLAWS ON FRACTURE BEHAVIOR OF STRUCTURAL CERAMICS

J.P. Singh, D. Singh, and M. Sutaria

Energy Technology Division
Argonne National Laboratory
Argonne, Illinois 60439

ABSTRACT

We evaluated the effects of fiber coating thickness, fiber orientation, and elevated temperature on flaw morphology and mechanical properties of Nicalon-fiber–reinforced SiC matrix composites with fiber cloth lay-up sequences of 0°/45, 0°/20°/60°, and 0°/40°/60° and fiber coating thicknesses of 0.2 and 0.4 μm. For the three fiber cloth lay-up sequences (0°/45°, 0°/20°/60°, and 0°/40°/60°), mechanical property (first matrix cracking stress, ultimate stress, and work of fracture) initially increase with coating thickness and reach peak values at a coating thickness of 0.2 μm. A further increase in coating thickness does not result in further improvements in mechanical properties; this is related to the role of coatings in protecting fibers from damage during composite processing. Measured values of strength and work-of-fracture of the above composites at elevated temperatures increased with temperature up to 1200°C, but decreased at higher temperatures. This decrease is correlated to in-situ fiber strength and fiber/matrix interface degradation.

Correlations between model prediction and measured room-temperature ultimate strength of composites with 0°/45° and 0°/40°/60° lay-up sequences were established by using in-situ fiber strength characteristics.

The failure modes and degradation mechanisms in hot-gas filters and ceramic composite joints are being characterized by the mechanical and fractographic evaluation techniques established thus far. Correlation of these results with those of nondestructive evaluation can provide critical information for improved quality control.

INTRODUCTION

Continuous fiber–reinforced ceramic matrix composites (CFCCs) are being pursued as materials for structural applications in various industries, including automotive, aerospace,

and utilities, chiefly because of their combination of high strength and toughness at both room and elevated temperatures.[1,2] It has now become clear that the mechanical response of CFCCs, for a fixed fiber content, is largely controlled by intrinsic composite parameters, including strengths of the reinforcing fibers and matrix,[3,4] fiber/matrix interface characteristics,[5,6] and fiber architecture. Therefore, effort is continuing on the evaluation of the effects of fiber cloth lay-up sequence, fiber/matrix interface, and high-temperature environments on flaw generation and resulting mechanical properties of reinforcing fibers and composites.

SPECIMEN FOR FRACTURE STUDIES

To evaluate the effects of fiber cloth lay-up sequence and elevated-temperature service environments on flaw generation and resulting mechanical properties, Nicalon-fiber-reinforced SiC matrix composites fabricated by chemical vapor infiltration (CVI) with various cloth lay-up sequences and fiber coating thicknesses were obtained from Ceramic Composites, Inc. (MD). To date, composites with fiber lay-up sequences of 0°/45°, 0°/20°/60°, and 0°/40°/60° and with carbon coating thicknesses of 0-0.4 μm have been evaluated. Fiber content in the final composite was ≈40 vol.%. These composites were received in plate form and used to machine rectangular bars (≈3 x 4 x 40 mm). The tensile edges of the test bars were bevelled to eliminate stress concentrations and thus avoid edge failures. Density was measured by the Archimedes principle. Approximately five specimens were tested per condition.

ROOM- AND ELEVATED TEMPERATURE MECHANICAL PROPERTY EVALUATIONS AND CORRELATIONS WITH FIBER ARCHITECTURE

Flexure testing in a four–point–bend mode was used to evaluate mechanical properties of the composites at room and elevated temperatures. This method was chosen because of its relatively low cost and ease of use. For room–temperature tests, flexural bars (2.9 x 4.2 x 25.4 mm) were tested with loading and support spans of 9.5 and 19.0 mm, respectively. All tests were conducted at a crosshead speed of 1.27 mm/min at ambient conditions on a universal testing machine.

High-temperature flexure tests were conducted at 1000, 1200, and 1300°C. The composite bars (2.9 x 4.2 x 28.0 mm) were similar to those tested at room temperature, except for an additional SiC surface coating (≈100 μm thick) to prevent oxidizing the exposed carbon

coating on the fiber surfaces. SiC fixtures with loading and support spans of 12.7 and 25.4 mm, respectively, were used, and crosshead speed was 1 mm/min. All specimens were loaded perpendicular to the mat layers. At least three specimens were tested under each set of conditions.

The first matrix cracking stress, or onset of permanent damage to the composites, was determined from the load at which first deviation from the linear variation in the load–vs.–displacement plots was observed. Nominal ultimate stress was determined from the peak load value. Composite work-of-fracture (WOF) was estimated from the total area under the load-specimen displacement plots normalized on the basis of unit cross-sectional area of the fractured composites. True specimen displacement was obtained by subtracting system displacement from total displacement (system displacement was determined by measuring system compliance with a stiff alumina piece).

ANALYTICAL BACKGROUND

Mechanical response of continuous fiber-reinforced ceramic matrix composites with increasing stress levels is dependent on in-situ fiber strength and its distribution. Based on the weakest-link-principle (i.e., failure occurs at the most severe flaw), strength distribution of fibers can be represented by the Weibull distribution function as follows:

$$F(\sigma) = 1 - \exp\left[-\frac{L}{L_o}\left(\frac{\sigma}{\sigma_o}\right)^m\right], \tag{1}$$

where $F(\sigma)$ is the cumulative failure probability at an applied stress σ, σ_o is the scale parameter signifying a characteristic fiber strength at a fiber gauge length, L_o, and m is referred to as the Weibull modulus that characterizes flaw distribution in the material. Thus, by using the Weibull distribution function as given by Eq. 1, it is possible to estimate Weibull scale parameter at some standard gauge length, L, with the following expression:

$$\sigma = \sigma_o\left(\frac{L_o}{L}\right)^{\frac{1}{m}}, \tag{2}$$

The in-situ fiber strength distribution parameters, σ_c and m, can be evaluated by measuring mirror sizes on fractured fibers. Figure 1 shows typical flaw morphology and

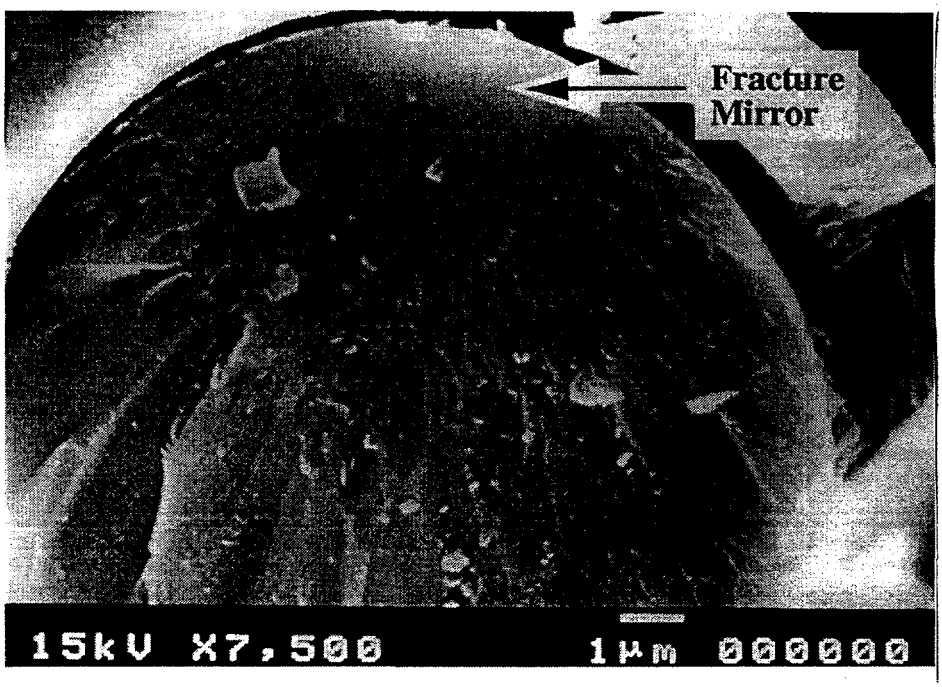

Fig. 1. Fracture surface morphology of SiC (Nicalon) fiber.

associated fracture features such as mirrors (smooth regions) and hackles (regions of multiple fracture planes) on a Nicalon fiber in a composite tested at room temperature. For brittle materials such as glasses and ceramics, it is possible to correlate sizes of fracture features to fracture stress with empirical relationships. For example, fracture stress, σ_f, of the fibers can be obtained from mirror-size measurements with the following relationship:[7]

$$\sigma_f = \frac{3.5K_f}{\sqrt{r_m}}, \tag{3}$$

where r_m is the mirror radius and K_f is the fracture toughness of the fiber. This semiempirical relationship is applicable for mirror sizes much smaller than the fiber diameter.

Based on the fiber fragmentation theory,[8] the resulting value of scale parameter, σ_c, from fracture mirror evaluations is at a gauge length, L_c, that is controlled by fiber/matrix interfacial shear strength and fiber strength. An average value for the gauge length for in-situ fractured fibers can be written as

$$L_c = r\frac{\sigma_c}{\tau}, \tag{4}$$

where r is the fiber radius and τ is the fiber/matrix interfacial shear strength.

The fiber/matrix interfacial shear strength can be determined from average fiber pullout length measurement, h, as[4,8]

$$\tau = \frac{\lambda(m)\, r\sigma_c}{4h}, \tag{5}$$

where $\lambda(m)$ is a nondimensional function and is dependent on fiber fracture statistics.

In-situ fiber strength distribution parameters (σ_c and m) can be correlated to the ultimate strength, σ_{UTS}, of the composite as follows:[8]

$$\sigma_{UTS} = f_l\sigma_c\left[\frac{2}{m+2}\right]^{1/m+1}\left[\frac{m+1}{m+2}\right], \tag{6}$$

where f_l is the fiber volume fraction parallel to the loading direction.

RESULTS AND DISCUSSION

As shown in Table 1, mechanical properties of composites are dependent on both fiber coating thickness and fiber cloth lay-up sequence. For sequences of 0°/45° and 0°/20°/60°, mechanical properties (first matrix cracking stress, ultimate stress, and work of fracture) initially increase with coating thickness and reach peak values at a coating thickness of 0.2 μm. Further increases in coating thickness do not result in further improvements in mechanical properties; this is believed to be related to the role of coating in protecting fibers from damage during processing and in service.[9] These results indicate an optimal coating thickness of 0.2 μm for fibers in the composites. Similar results have been obtained for CVI SiC/SiC composites obtained from Oak Ridge National Laboratory.[9]

Table 1. Room-temperature mechanical property data for SiC/SiC CFCC with various different fibercloth lay-up sequences

Fiber Architecture	Coating Thickness (μm)	Composite Density g/cm^3)	First Matrix Cracking Stress (MPa)	Ultimate Stress (MPa)	Work-of-Fracture (kJ/m^2)
0°/45°	0.0	-	-	105 ± 28	0.16
	0.2	-	95.0	321 ± 131	17.8 ± 6
	0.4	2.25	86 ± 23	153 ± 41	9.8 ± 2
0°/20°/60°	0.0	2.43	-	93 ± 12	0.25 ± 0.6
	0.2	2.31	223 ± 15	319 ± 41	12.7 ± 2.3
	0.4	2.40	115 ± 25	287 ± 48	15.7 ± 4
0°/40°/60°	0.4	2.46	116 ± 28	312 ± 28	14.4 ± 4

For a given fiber coating thickness, mechanical properties of composites with 0°/20°/60° and 0°/40°/60° fiber lay-up sequences were similar in magnitude, whereas composites with fiber a sequence of 0°/45° had relatively lower values. The decrease in mechanical properties for composites with the 0°/45° sequence is believed to have two causes: first, composites with a fiber lay-up sequence of 0°/45° had a lower density (2.25 g/cm^3) than composites with other fiber lay-up sequences (Table 1); the second cause could be related to the smaller fiber fraction in the loading direction for 0°/45° composites relative to that of composites with other fiber lay-up sequences. This will be discussed in more detail in the following sections.

Figure 2 shows typical load-displacement behavior obtained from flexure tests conducted on SiC(f)/SiC composites with the 0°/40°/60° fiber lay-up sequence, at both room and elevated temperatures. Similar variations in load displacement were observed for the 0°/45° composites, and gradual failure was observed in all tests. However, the area under the curve increased somewhat in tests at elevated temperatures. It is recognized here that because of the generation of matrix crack(s) and the shift in the neutral axis, use of the simple beam theory to assess ultimate stresses gives a semiquantitative estimate of ultimate strength. However, the purpose of estimating these values is to compare the relative load-bearing properties of the composites under specific fiber orientations and test conditions.

Figure 3 shows the variation of ultimate strength for the three sets of composites (0.4 μm coating thickness) as a function of temperature. At 1000°C, strength of the 0°/40°/60° composites was similar to its room-temperature value. No 0°/45 specimens were available for tests at 1000°C. Beyond 1000°C, the ultimate strengths of both sets of composites increased dramatically over their room-temperature values, probably because of matrix-softening effects at elevated temperatures. Such behavior is well documented in monolithic ceramics and CFCCs.[10] In general, at elevated temperatures, the 0°/40°/60° composites had higher strengths than those of the 0°/45° composites. However, at 1300°C, strengths of both sets of composites dropped to ≈270 MPa. This decrease above 1200°C is believed due to degradation in strength of the reinforcing fibers.[11-13] For the 0°/20°/60° composites, strength remained relatively unchanged up to 1300°C, except for a slight decrease at 1200°C.

Observed WOF variation with test temperature of two sets of composites (0°/45° and 0°/40°/60°) was similar (see Fig. 4). With increasing test temperature, WOF increased to a maximum at 1200°C because of matrix-softening effects, but dropped rapidly above 1300°C. This drop is related to physical changes in the in-situ Nicalon fibers in composites tested at elevated temperatures; formation of silica at the fiber surface is a distinct possibility at elevated temperatures and can lead to degradation of fiber/matrix interfacial properties. This oxidation can minimize the effective fiber pullout during fracture of the composites, thus accounting for low WOF values.[14]

However, for 0°/20°/60° composites, the WOF remained relatively unchanged up to 1300°C, except for a slight decrease at 1200°C. This behavior is consistent with the observed strength behavior. The difference in mechanical behavior of 0°/20°/60° composites from that of 0°/40°/60° and 0°/45° composites is probably due to specimen-related variations.

To establish the large difference in room-temperature strengths of 0°/40°/60° and 0°/45° composites, we measured their in-situ fiber strengths and correlated them to the composite strengths. In-situ fiber strength measurements by fractography were made on the two sets of composites samples fractured at room temperature. In most fibers, fractures originated at surface flaws, as shown in Fig. 1. Using mirror size measurements and a value of 1 MPa$\sqrt{m}$ as the Nicalon fiber fracture toughness,[4] we estimated fiber strengths from Eq. 3; these values were then used to construct linearized Weibull plots with Eq. 1.

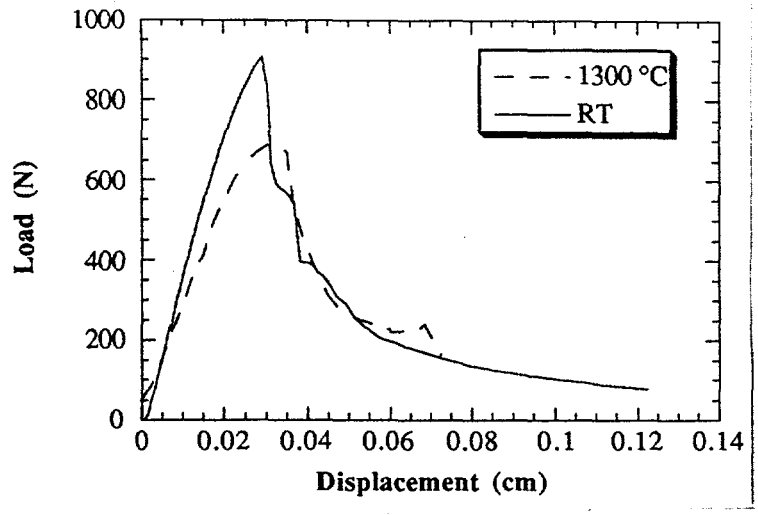

Fig. 2. Typical Load Displacement Observed for 0°/40°/60° Composites Tested at Room Temperature and 1300°C.

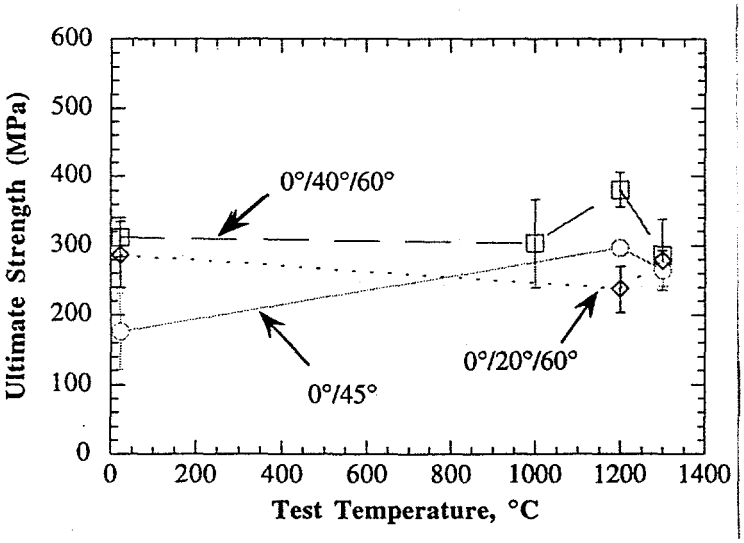

Fig. 3. Variation of ultimate strength with test temperature for SiC(f)/SiC composites with different fiber lay-up sequences.

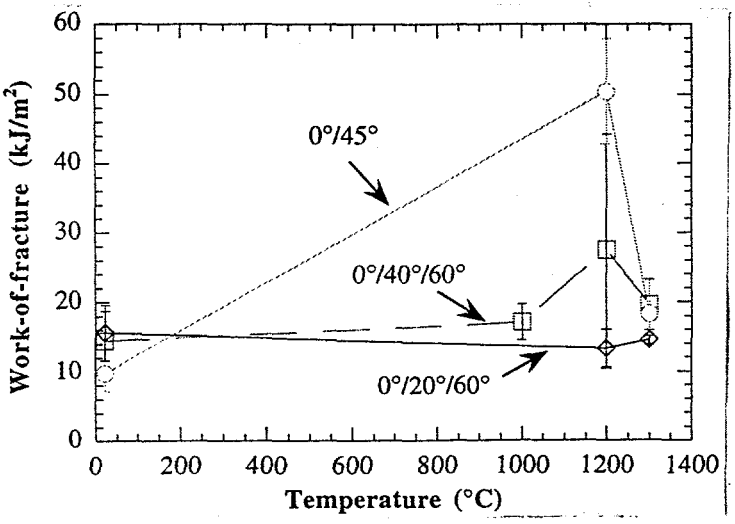

Fig. 4. Variation of work-of-fracture with test temperature for SiC(f)/SiC composites with different fiber lay-up sequences.

The linearized Weibull plots (not shown) of in-situ fibers in 0°/40°/60° and 0°/45° composites tested at room temperature were used to estimate the scale perameter and Weibull modulus. These values for the 0°/40°/60° composites were 2.42 and 4.9 GPa, respectively, while those for the 0°/45° composites were 2.38 and 4.9 GPa, respectively. Associated average fiber pullout lengths were 160 μm for the 0°/45° and 200 μm for the 0°/40°/60° composites.

For comparison purposes, the scale parameters for fractured fibers in the 0°/40°/60° and 0°/45° composites tested at room temperature were evaluated at a standard gauge length of 1 mm. This was done by first estimating the gauge length, L_c, for the fractured fibers in the composites tested with the two fiber lay-up sequences, based on the average fiber pullout lengths and the scale parameters (Eq. 4). Fiber radius was assumed to be 8 μm, and λ was taken as 2.1 for fibers tested in both 0°/40°/60° and 0°/45° composites.[8] The corresponding values for the gauge lengths of fractured fibers were estimated as 381 and 305 μm for the 0°/40°/60° and 0°/45° composites, respectively. Subsequently, these fiber gauge lengths were used in conjunction with Eq. 2 to estimate scale parameters for the in-situ fibers at a gauge length of 1 mm. The resulting scale parameters at a gauge length of 1 mm for in-situ fractured fibers in the 0°/40°/60° and 0°/45° composites tested at room temperature were 2 and 1.87 GPa,respectively. These values were then used to plot Weibull distribution curves (Fig. 5). Similarity in the Weibull strength distribution plots suggests that there are no differences in in-situ fiber strength characteristics for the two sets of composites.

Equation 6 was used to determine the ultimate strengths of the 0°/40°/60° and 0°/45° composites tested at room temperature. As a first approximation, the fraction of fibers along the loading direction (i.e., 0°) are accounted for in the calculations. Therefore, values of f_l for the 0°/40°/60° and 0°/45° composites are 0.07 and 0.1, respectively. Based on these values and the Weibull parameters, predicted ultimate strengths for the 0°/40°/60° and 0°/45° composites are 117 and 165 MPa. The predicted strength for the 0°/45° composites agrees well with the observed room-temperature strength of ≈153 MPa, while for the 0°/40°/60° composites, there is a large discrepancy. It is possible that in the 0°/40°/60° composites, fibers in the lay-ups oriented at 40° and 30° (in 60° oriented mats) may be contributing to the mechanical response of the composite. If the contribution of these fibers is included in the model, the predicted strength for the 0°/40°/60° is ≈334 MPa; this is in accordance with the observed strength of ≈312 MPa. Thus, from this work it seems that fibers oriented off-axis by more than 45° do not contribute significantly to the ultimate strength of the composites. However, if they are

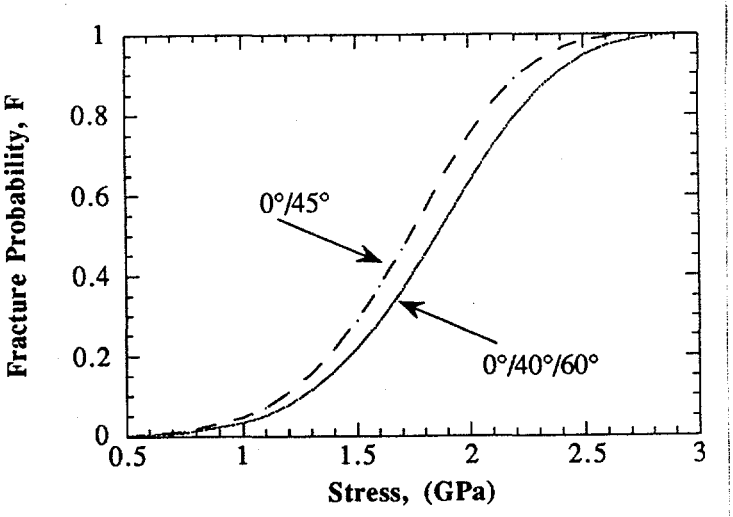

Fig. 5. Weibull strength distribution of in-situ Nicalon fibers in 0°/40°/60° and 0°/45° composites at gauge length of 1 mm.

oriented <40° from the loading direction, they do influence composite strength. Realistically, the contribution of the off-axis fibers to composite strength is expected to change gradually with the off-axis angle and needs to be further quantified. In addition to the fiber fraction available to sustain the applied loads, there may also be a change in the failure mechanism as the fiber lay-up sequence changes in the composites.

ENGINEERING APPLICATIONS

These techniques are currently being used to provide insight into the effects of in-situ fiber strength, fiber coating, and fiber architecture on mechanical performance of engineering composites in service environments. We have begun to investigate engineering components and processes being developed for commercial applications. Specifically, damage evaluation of composite hot-gas filters exposed to service environments and composite joints has been conducted.

Composite Hot-Gas Filters

O-ring compression tests on samples machined from composite hot-gas filters in as-fabricated condition showed an ultimate strength of 19.7 ± 2 MPa. The corresponding value for the ultimate strength of a filter exposed in the Tidd demonstration plant for ≈1100 h was 7.7 ± 1 MPa. This represents a strength loss of 60% during filter exposure. Based on observations in other studies,[15,16] we believe that the reduced ultimate strength is related to the degradation of in-situ fiber strength. Therefore, we evaluated the in-situ strength of reinforcing fibers in as-fabricated and exposed filters by using the fractographic technique

discussed above. Figure 6 shows the distribution of in-situ fiber strengths in composite filters in both as-fabricated and exposed conditions. The average fiber strength in as-fabricated filters is ≈1.7 GPa, while that in exposed composite filter is ≈0.8 GPa. Thus, fiber strength reduction during exposure is a≈60%, in agreement with the strength degradation of the filters themselves. This confirms that filter strength degradation is related to fiber damage.

Composite Joining

An evaluation of in-situ fiber strength in an as-fabricated composite and in a lap joint made of the same composite showed significant fiber strength degradation in the joint section. This is consistent with the observed strength degradation of composite joints. These results validate the use of in-situ fiber strength evaluation for damage evaluation that leads to process optimization of engineering composite components.

ACKNOWLEDGMENTS

The work was supported by the U.S. Department of Energy, Office of Fossil Energy, Advanced Research and Technology Materials Program [DOE/FE AA 15 10 10 0, Work Breakdown Structure Element ANL-1], under Contract W-31-109-Eng-38. The authors thank

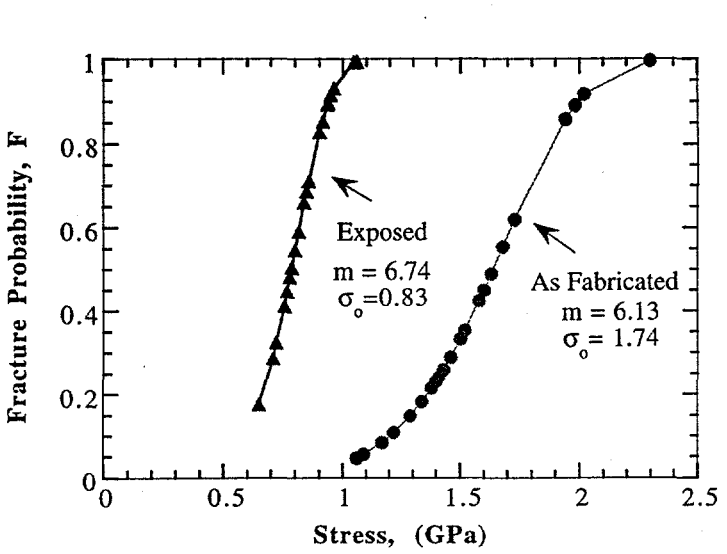

Fig. 6. Weibull strength distribution of in-situ fibers in composite hot gas filters before and after exposure in Tidd demonstration plant.

D. J. Pysher, B. L. Weaver, and R. G. Smith of the 3M Company for providing filter specimens, and James K. Weddel from DuPont Lanxide for providing the composite joint specimen.

REFERENCES

1. A. G. Evans and D. B. Marshall, "The Mechanical Behavior of Ceramic Matrix Composites," Overview No. 85, Acta Metall., 37 [10] 2567–2583 (1989).

2. E. Y. Luh and A. G. Evans, "High–Temperature Mechanical Properties of a Ceramic Matrix Composite," J. Am. Ceram. Soc., **70** [7] 466–69 (1987).

3. T. Mah, M. G. Mendiratta, A. P. Katz, R. Ruh, and K. S. Mazdiyasni, "Room–Temperature Mechanical Behavior of Fiber–Reinforced Ceramic–Matrix Composites," J. Am. Ceram. Soc., **68** [1] C–27–C–30 (1985).

4. M. D. Thouless, O. Sbaizero, L. S. Sigl, and A. G. Evans, "Effect of Interface Mechanical Properties on Pullout in a SiC–Fiber–Reinforced Lithium Aluminate Silicate Glass Ceramic," J. Am. Ceram. Soc., **72** [4] 525–32 (1989).

5. H. C. Cao, E. Bishcoff, O. Sbaizero, M. Ruhle, A. G. Evans, D. B. Marshall, and J. J. Brennan, "Effect of Interfaces on the Properties of Fiber–Reinforced Ceramics," J. Am. Ceram. Soc., **73** [6] 1691–99 (1990).

6. R. N. Singh, "Fiber–Matrix Interfacial Characteristics in a Fiber–Reinforced Ceramic–Matrix Composite," J. Am. Ceram. Soc., **72** [9] 1764–67 (1989).

7. R. W. Rice, Treatise on Materials Science and Technology, Vol. II, pp. 199, Academic Press, New York, 1978.

8. W. A. Curtin, "Theory of Mechanical Properties of Ceramic–Matrix Composites," J. Am. Ceram. Soc., **74** [11] 2837–45 (1991).

9. J. P. Singh, D. Singh, and R. A. Lowden, "Effect of Fiber Coating on Mechanical Properties of Nicalon Fibers and Nicalon-Fiber/SiC Matrix Composites," Ceram. Eng. Sci. and Proc., **15** [4] 456–464 (1994).

10. D. P. Stinton, R. A. Lowden, and R. H. Krabill, "Mechanical Property Characterization of Fiber-Reinforced SiC Matrix Composites," in Proc. 4th Annual Conf. on Fossil Energy Materials, Fossil Energy AR&TD Materials Program, ORNL/FMP-90/1, 3-13 (1990).

11. D. Singh, J. P. Singh, and M. Wheeler, "Mechanical Behavior of SiC(f)/SiC Composites and Correlation to In-Situ Fiber Strength at Room and Elevated Temperatures," to appear in Journal of the American Ceramic Society.

12. T. J. Clark, R. M. Arons, and J. B. Stamatoff, "Thermal Degradation of Nicalon SiC Fibers," Ceram. Eng. Sci. Proc., **6** [7-8] 576-588 (1985).

13. D. J. Pysher, K. C. Goretta, R. S. Hodder, and R. E. Tressler, "Strengths of Ceramic Fibers at Elevated Temperatures," J. Am. Ceram. Soc., **72** [2] 284–88 (1989).

14. R. A. Lowden and D. P. Stinton, "Interface Modification in Nicalon/SiC Composites," Ceram. Eng. Sci. Proc., **9** [7-8] 705-722 (1988).

15. J. P. Singh, D. Singh, and R. A. Lowden, "Effect of Fiber Coating on Mechanical Properties of Nicalon Fibers and Nicalon-Fiber/SiC Matrix Composites," Ceram. Eng. Sci. Proc., Vol. 15, [4] 456-464 (1994).

16. D. Singh and J. P. Singh, "Effect of Processing on Strength of Nicalon Fibers in Nicalon Fiber-SiC Matrix Composites", Ceram. Eng. Sci. Proc., Vol. 13, [7-8] 257-266 (1992).